Vol. 46 No. 5 SCIENCE IN CHINA (Series B) October 2003

A theoretical study on nitration mechanism of benzene and solvent effects

XIAO Heming (肖鹤鸣)[1], CHEN Litao (陈丽涛)[1,2], JU Xuehai (居学海)[1]
& JI Guangfu (姬广富)[1]

1. Department of Chemistry, Nanjing University of Science & Technology, Nanjing 210094, China;
2. Institute of Chemical Engineering, Zhejiang University of Technology, Hangzhou 310014, China
Correspondence should be addressed to Xiao Heming (email: xiao@mail.njust.edu.cn)

Received June 3, 2003

Abstract Both π and σ transition states on the potential energy surface of the nitration of benzene with nitronium ion have been successfully optimized using unrestricted hybrid DFT procedure B3LYP with the triple-zeta 6-311G** basis set without any assumption. Subsequently, a σ reactant-complex and a σ intermediate (Wheland intermediate) were located by the intrinsic reaction coordinate (IRC) calculation. The reaction pathway and the experimental observation lacking the kinetic isotopic effect in the title nitration were confirmed on geometries, atomic charges, energies, IR spectra and thermodynamic properties of all stationary points. The activation energy of 8.370 kJ/mol in the gas phase and the order of 10^{10} mol • L^{-1} • s^{-1} of rate constant were obtained for the reaction. The results both in thermodynamics and kinetics show that the electrophilic substitute mechanism is more preferable than the electron transfer mechanism of radical pairs. The solvent effect on the geometries of stationary points and the reaction mechanism were systematically studied for the nitration of benzene with nitronium by self-consistent reaction field (SCRF) technique with different dielectric constants of 5.0, 25.0, 50.0 and 78.5. It was then found that the solvent effect would depress the activation energy and finally make the formation of σ-TS without energy barrier in aqueous solution. Furthermore, the linear correlations given by charge migrations of NO_2 group, dipole moments of solute, gaps of HOMO and LUMO and solvent stabilization energies in different solvents were demonstrated for both theoretically and experimentally concerned Wheland intermediate.

Keywords: benzene, nitronium ion, nitration mechanism, solvent effect, density functional theory.

DOI: 10.1360/02yb0215

Aromatic nitration is an important and canonical example of electrophilic substitution in organic chemistry. The research on nitration mechanism is also very important for synthesis of explosives since benzene molecule is a basic unit to build up into the energetic material. Besides the electrophilic substitution mechanism, there is an electron transfer mechanism[1,2]. The nitronium ion (NO_2^+), however, is a generally accepted active nitrating agent in the aromatic nitration. Therefore, the nitration of aromatics with nitronium is still an active area[1—10] for both experimental and theoretical investigations. Theoretically, Politzer et al.[4] have computed the properties of some possible intermediate stages in the reactions of benzene and toluene with NO_2^+ by freezing the N-O bond lengths of NO_2 group at the HF/STO-6G and HF/5-31G levels. Gleghorn[5] has located five benzene-NO_2^+ complexes by HF/STO-3G, yet no connections, in terms of pathway, were involved for these five complexes. In 1992, Szabo et al.[6] finally obtained two energy profiles for the nitration of benzene with the possible protonated methyl nitrate isomers also by incomplete optimization, freezing the distance between the attacked carbon atom and the nitrogen atom of nitronium ion while optimizing the rest of the internal coordinates within stationary points of the reaction profile simultaneously at the HF/3-21G level. The structure of transition state for benzene with bare (unsolvated) nitronium ion, however, could not be reached because the plot of single point energy vs. the distance of C-N simply increases. In a word, the confirmation of electrophilic substitute trajectory for the aromatic nitration is still a difficult problem.

Based on our knowledge and working experience in nitro compounds, some with benzene ring[11—15], we recently finished the full optimization for the complexes of stationary points, including two transition states (σ-TS and π-TS), one reactant (σ-R) and one intermediate called Wheland intermediate (σ-INT) by employing unrestricted hybrid DFT procedure B3LYP[16], and then obtained the information about geometries, atomic charges, energies, IR frequencies and intensities, as well as standard thermodynamic functions (H_{m}^{0}, $C_{\mathrm{p,m}}^{0}$ and S_{m}^{0}) in the region of 200—800 K of all stationary points for the titled nitration. This is helpful for us to illustrate the microscope picture about the nitration pathway. Considering that a nitration is usually happened in a solution, we systematically computed the properties of all stationary points in different media by self-consistent reaction field (SCRF) technique with different dielectric constants, and finally evaluated the solvent effect on the nitration by comparing the behavior in both gas phase and solutions.

1 Computational methods and details

Simulating a system with nitro and benzyl group together usually requires high-level computational resources because there are strong electron correlations in this conjugated system. Yet many earlier theoretical works had been halted by either semiempirical calculation or low level of Hartree-Fock (HF) theory for the limitations both in computer and program. Incomplete optimizations and failures in locating a transition state with flat activation barrier often appeared in those early works. In this paper, however, two transition states (σ-TS and π-TS) were successfully optimized by the practical B3LYP hybrid DFT method, which is good at the simulation on a conjugated system with strong polarization and correlation effects, with 6-311G** basis set. We also benefit by the trick for locating a transition state with flat barrier in Gaussian 98 procedure[17]. These two transition states were all finally identified with only one imaginary frequency by the vibration analysis for a real saddle on the potential surface of reaction. The geometries of reactant (σ-R) and intermediate (σ-INT) were consequently obtained by the intrinsic reaction coordinate (IRC) analysis and also positively identified with no imaginary frequencies for a real minimum on the potential surface.

The simulation of solvent effect is based on the Onsager self-consistent reaction field (SCRF)[18] technique, which supposes that the solute molecule is embedded into a spherical cavity with radius a_0 surrounded and the solvent is represented by a continuous dielectric, characterized by a given dielectric constant (ε). A dielectric constant used for the SCRF calculations in a big value represents a strongly polar medium. Contrarily, a dielectric constant under 5.0 stands for a nonpolar medium. A dipole moment of solvent, induced by that of the solute, interacts back to the dipole moment of solute to gain the stabilization energy for the system. The gas-phase geometry of each complex was used as its initial guess to start the full optimizations at the same level of B3LYP/6-311G** with different dielectric constants of 5, 25, 50 and 78.5 and a radius a_0 automatically resorted from quantum mechanical procedures. Totally 16 stationary points ($4\times4=16$) were all identified again for a minimum on the profile with no imaginary frequencies and a transition state with only one imaginary frequency. All works were finished on our Alpha workstation and Petium-IV personal computer.

2 Results and discussion

2.1 Geometries and solvent impacts

The numbering for four complexes is the same as that shown in fig. 1. Some of their geometries and bond orders in gas phase and different media are listed in table 1. As seen in table 1, only three of C-C bond lengths in benzene ring are shown there because the left three can be known by the roughly C_{2v} symmetry of complexes. None of the bond angles within the ring appears in table 1 because they vary insignificantly, ranging from 119° to 122°, while NO_2^+ attacks. The angle α ($O_{14}N_{13}O_{15}$) of NO_2 group is shown there.

Experimentally, whether the nitration rate varies with a heavier isotopic substitution of deuterium or tritium for the hydrogen in benzene or not is usually used to judge if the C-H bond cleaves at the rate-determining step or not. The elimination of D^+ or T^+ should be approximately 10 or 20 times slower than that of H^+, and the vibrational frequencies of bond C-H, C-D and C-T are different. Yet, there is no isotope effect in most aromatic nitrations. For example, in H_2SO_4 solution the nitration rate of nitrobenzene is the same as that of perdeuterated nitrobenzene. And the nitration rate of either perdeuterated or tritiated benzene, toluene or naphthalene is the same as that of its own. This shows that the cleavage of C-H bond is not happened at the rate-determining step, the electrophilic addition step, but the fast one in which the Wheland intermediate becomes a product of nitro compound and a proton.

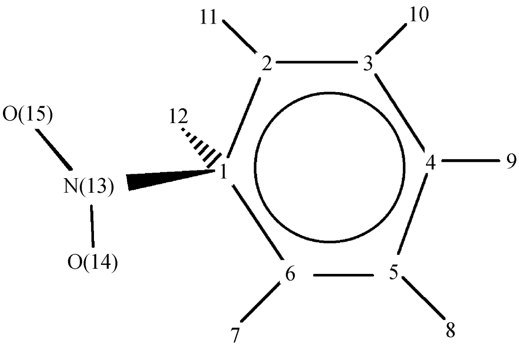

Fig. 1. Numbering for complexes.

Comparing the bond length and its corresponding bond order for C_1-H_{12} and C_1-N_{13} on going

Table 1 Some bond lengths (r), bond angles (α), dihedral angles (β) and bond orders (bo) of complexes in vacant and different media (bond length in pm; angle in (°)) at B3LYP/6-311G** level

		r(C_1-N_{13})	r(C_1-H_{12})	r (C_1-C_2)	r (C_2-C_3)	r (C_3-C_4)	r (N_{13}-O_{15})	α (O_{14}-$N_{13}O_{15}$)	β ($O_{15}N_{13}$-C_1H_{12})	bo(C_1-N_{13})	bo(C_1-H_{12})
$\varepsilon = 1$	π-TS	235.4	108.4	139.9	138.4	142.1	116.5	142.7	–23.1	0.0564	0.4208
	σ-R	209.7	108.3	143.6	137.4	140.9	117.1	139.5	0.0	0.1405	0.4079
	σ-TS	182.6	109.1	145.7	137.2	140.7	118.6	134.0	49.6	0.1489	0.3911
	σ-INT	161.4	111.1	146.8	136.7	141.2	120.1	130.0	88.8	0.1283	0.3455
$\varepsilon = 5$	π-TS	234.5	108.4	140.0	138.3	142.1	116.7	142.3	–22.0	0.0570	0.4206
	σ-R	203.2	108.3	144.1	1.372	141.1	117.6	137.7	0.0	0.1465	0.4060
	σ-TS	176.6	108.9	146.6	136.7	141.2	119.2	132.2	25.3	0.1612	0.3938
	σ-INT	157.4	111.4	147.4	136.5	141.5	120.8	128.1	88.7	0.1391	0.3346
$\varepsilon = 25$	π-TS	234.1	108.4	140.0	138.3	142.1	116.7	142.0	–22.9	0.0571	0.4206
	σ-R	199.4	108.3	144.3	137.1	141.3	117.9	136.7	–3.8	0.1493	0.4049
	σ-TS	175.6	108.8	146.7	136.5	141.5	119.4	131.7	4.2	0.1665	0.3939
	σ-INT	156.7	111.4	147.6	136.5	141.6	121.0	127.5	88.6	0.1432	0.3324
$\varepsilon = 50$	π-TS	234.1	108.4	140.0	138.3	142.1	116.7	142.0	–22.9	0.0571	0.4205
	σ-R	198.2	108.3	144.4	137.0	141.3	117.9	136.4	–4.2	0.1500	0.4045
	σ-TS	176.8	108.7	146.6	136.5	141.5	119.4	132.0	0.0	0.1654	0.3951
	σ-INT	156.6	111.4	147.6	136.5	141.6	121.1	127.4	88.6	0.1437	0.3322
$\varepsilon = 78.5$	π-TS	234.1	108.4	140.0	138.3	142.1	116.7	142.0	–22.9	0.0571	0.4205
	σ-R	198.2	108.3	144.4	137.0	141.3	117.9	136.4	–4.2	0.1501	0.4045
	σ-TS	156.2	110.7	148.2	136.2	141.7	121.1	127.9	0.0	0.1888	0.3317
	σ-INT	156.6	111.4	147.6	136.5	141.6	121.1	127.4	88.6	0.1439	0.3321

from π-TS to σ-R to σ-TS to σ-INT in any medium, it is evident that the r(C_1-H_{12}) lengthens very little and its bond order decreases also slightly while the reaction proceeds forward. This suggests that the C_1-H_{12} bond is still very strong and would not cleave during the formation step of Wheland intermediate, which is in a good agreement with the experimental observation of the absence of kinetic isotopic effect in most aromatic nitration reactions. Contrarily, the r(C_1-N_{13}) simply shortens from π-TS toward σ-INT, showing that the interaction between carbon and nitrogen gets stronger along the pathway and the C_1-N_{13} bond is partially formed in the σ-INT. However, the bond order of C_1-N_{13} increases on going from π-Ts to σ-R to σ-TS, but decreases from σ-TS to σ-INT. This shows that the electrostatic interaction, rather than covalent orbital overlap, between benzene ring and NO_2 moiety becomes stronger while the process reaches σ-INT, which meets the experimental observation of the carbocation character of Wheland intermediate.

Viewing the data in table 1, the solvent effects on the geometries of benzene ring in four complexes of stationary points are insignificant since those rings are almost in the same resonance structure in solvents as they are in gas phase. The bond C_1-N_{13}, however, is the most heavily influenced by solvents both in bond length and bond order, especially in the complexes of σ-TS and σ-INT whose dipole moment is significant (see table 2). The bond C_1-N_{13} shortens while the solvent polarity increases. And in aqueous solution the bond length of C_1-N_{13} in σ-TS is very close to that in σ-INT, showing that the σ-TS is a typical later transition state in aqueous medium. Its bond

Table 2 Energetics and the dipole moments of four complexes in different media at B3LYP/6-311G** level

	Species	E_T (a.u.)	E_T (Z)(a.u.)	$\Delta E_{solv}(Z)$ /kJ • mol^{-1}	$\Delta E_R(Z)$ /kJ • mol^{-1}	Gap (a.u.)	Dip/D
$\varepsilon = 1$	π-TS	–437.13205	–437.01993	0.0	2.744	0.1114	0.777
	σ-R	–437.13357	–437.02098	0.0	0.0	0.1192	1.788
	σ-TS	–437.13008	–437.01779	0.0	8.370	0.1319	4.290
	σ-INT	–437.13266	–437.02008	0.0	2.355	0.1429	6.581
$\varepsilon = 5$	π-TS	–437.13214	–437.02013	–0.522	3.888	0.1118	1.025
	σ-R	–437.13411	–437.02161	–1.667	0.000	0.1225	2.710
	σ-TS	–437.13290	–437.02056	–7.265	2.773	0.1347	5.620
	σ-INT	–437.14082	–437.02812	–21.10	–17.08	0.1484	8.684
$\varepsilon = 25$	π-TS	–437.13218	–437.02024	–0.811	4.448	0.1119	1.131
	σ-R	–437.13438	–437.02194	–2.515	0.000	0.1243	3.248
	σ-TS	–437.13403	–437.02173	–10.344	0.003	0.1358	5.985
	σ-INT	–437.14421	–437.03150	–29.98	–25.11	0.1498	9.428
$\varepsilon = 50$	π-TS	–437.13219	–437.02023	–0.764	4.645	0.1119	1.147
	σ-R	–437.13443	–437.02199	–2.665	0.000	0.1249	3.395
	σ-TS	–437.13419	–437.02190	–10.796	0.239	0.1352	5.861
	σ-INT	–437.14471	–437.03202	–31.33	–26.31	0.1500	9.536
$\varepsilon = 78.5$	π-TS	–437.13219	–437.02023	–0.775	4.694	0.1119	1.153
	σ-R	–437.13445	–437.02202	–2.725	0.000	0.1249	3.405
	σ-TS	–437.13554	–437.02310	–13.926	–2.830	0.1471	9.149
	σ-INT	–437.14490	–437.03221	–31.83	–26.75	0.1501	9.576

order declines from σ-TS to σ-INT in any medium (vide ante). The dihedral angle of $\beta(O_{15}\text{-}N_{13}C_1H_{12})$ is drastically changed from 0.0º to 88.6º in aqueous solution. That is, the plane of NO_2 is vertical, rather than parallel, to an imaginary line of $C_1 \cdots C_4$.

The structure of NO_2^+ is initially linear, but bents in all four complexes. The bond N-O lengthens but the angle $\alpha\,(O_{14}N_{13}O_{15})$ decreases on going from π-TS to σ-INT in any medium. And the impact of solvent on these two bond parameters is that the more they are changed in magnitude, the larger polar solvent their complex is in. That is, for a complex the bond N-O lengthens while the bond angle of NO_2 decreases on going from gas phase to non-polar solvent to aqueous solution.

2.2 Charge migrations and solvent impacts

Considering the symmetry of complexes, only some computational results on atomic charges, as well as the charge of NO_2 group of four stationary points at B3LYP/6-311G** level are listed in table 3. As an electronic acceptor, the NO_2^+ attacks the electron-rich benzene ring by its vacant 2p orbit to form an electron donor-acceptor complex. From the last column of table 3, about the charge migration of NO_2 group, it is evident that the net charge in NO_2 moiety is gradually neutralized on going from π-TS to σ-R to σ-TS to σ-INT. In gas phase, for example, the charge of NO_2 group of these four complexes is 0.340, 0.273, 0.110 and –0.049e respectively, showing that an electron has been migrated to the NO_2 moiety in σ-INT, and a carbocation intermediate (Wheland) is then formed. Charge migration like this is much different from the electron transfer

Table 3 Some atomic charges and the charge of NO_2 group of four stationary points in different media at B3LYP/6-311G** level

		C_1	C_2	C_3	C_4	H_{12}	H_{11}	H_{10}	H_9	N_{13}	O_{14}	NO_2
$\varepsilon = 1$	π-TS	–0.129	–0.018	–0.048	–0.048	0.189	0.165	0.171	0.171	0.393	–0.028	0.340
	σ-R	–0.280	0.040	–0.076	0.003	0.208	0.176	0.168	0.179	0.377	–0.056	0.273
	σ-TS	–0.239	0.043	–0.055	–0.004	0.253	0.197	0.173	0.189	0.320	–0.108	0.110
	σ-INT	–0.118	0.001	–0.039	–0.003	0.275	0.208	0.179	0.196	0.288	–0.168	–0.049
$\varepsilon = 5$	π-TS	–0.127	–0.016	–0.046	–0.046	0.190	0.166	0.172	0.172	0.386	–0.033	0.324
	σ-R	–0.277	0.049	–0.073	0.011	0.212	0.177	0.173	0.186	0.356	–0.073	0.215
	σ-TS	–0.219	0.048	–0.044	0.008	0.241	0.192	0.181	0.204	0.297	–0.138	0.030
	σ-INT	–0.092	–0.007	–0.032	0.013	0.277	0.202	0.195	0.224	0.267	–0.202	–0.138
$\varepsilon = 25$	π-TS	–0.126	–0.016	–0.046	–0.046	0.190	0.166	0.173	0.173	0.383	–0.035	0.317
	σ-R	–0.273	0.052	–0.071	0.015	0.215	0.177	0.175	0.190	0.344	–0.083	0.182
	σ-TS	–0.210	0.044	–0.040	0.014	0.232	0.186	0.184	0.208	0.296	–0.147	0.011
	σ-INT	–0.087	–0.010	–0.029	0.020	0.277	0.199	0.201	0.234	0.261	–0.213	–0.165
$\varepsilon = 50$	π-TS	–0.126	–0.015	–0.046	–0.046	0.190	0.166	0.173	0.173	0.383	–0.035	0.316
	σ-R	–0.271	0.053	–0.070	0.016	0.216	0.178	0.176	0.191	0.341	–0.086	0.173
	σ-TS	–0.216	0.044	–0.042	0.015	0.231	0.184	0.184	0.208	0.298	–0.144	0.019
	σ-INT	–0.086	–0.011	–0.029	0.020	0.277	0.198	0.202	0.236	0.261	–0.215	–0.169
$\varepsilon = 78.5$	π-TS	–0.126	–0.015	–0.046	–0.046	0.190	0.166	0.173	0.173	0.383	–0.036	0.316
	σ-R	–0.271	0.053	–0.070	0.016	0.216	0.178	0.176	0.191	0.341	–0.086	0.172
	σ-TS	–0.271	0.053	–0.026	0.017	0.216	0.178	0.197	0.229	0.245	–0.210	–0.167
	σ-INT	–0.086	–0.011	–0.029	0.021	0.277	0.198	0.202	0.237	0.260	–0.215	–0.170

mechanism of radical pairs in which an electron is transferred from NO_2^+ to benzene to form radical pairs of benzyl cation and NO_2. However, no spin densities appeared in either moiety of benzene or NO_2 group in complexes when the unrestricted B3LYP was employed to locate the geometries of all stationary points in any medium, showing that there is no any sights of unpaired single electron and radical character in these complexes. Instead, the bond C_1-N_{13} is partly formed by the interaction between two moieties bit by bit while the NO_2^+ closes to the benzene ring.

For each complex, the positive charge of NO_2 group is neutralized more while the solvent polarity increases, especially on going from gas phase to the nonpolar solvent of $\varepsilon = 5$. After that, on going from a solvent of $\varepsilon = 25$ to an aqueous solution, the magnitude of atomic charge is almost unchanged. The σ-TS, however, is an exception, the charge of NO_2 group changes from 0.019 e to –0.167e, which is very close to that of σ-INT, –0.170e, while the dielectric constant of solvent varies from 50 to 78.5. This indicates again that the σ-TS is truly a later transition state, and the polar solvent could strengthen the interaction between the benzene and NO_2 moieties and promote the charge migration from one part to another.

Viewing the atomic charge distributions of four stationary points in solvents it is found that the atomic charges in the π-TS vary the least while the dielectric constant changes because its dipole moment is the smallest one among the four (see table 2). Contrarily, in the dipole moment largest σ-INT, the atomic charges vary the most significantly while the solvent dielectric constant changes. For example, the charge of NO_2 group in σ-INT has dropped 0.089 e, from –0.049 to –0.138, on going from gas phase to the nonpolar medium of $\varepsilon = 5$.

2.3 Energetics, reaction mechanisms and solvent impacts

The energetics and the dipole moments (Dip) of four complexes in different media at B3LYP/6-311G** level are listed in table 2. The E_T is the total energy and $E_T(Z)$ the total energy including ZPVE correction. The $\Delta E_{solv}(Z)$ is the stabilization energy by solvents, the relative energy of a complex in a solvent to that in the gas phase. The $\Delta E_R(Z)$ then is the relative energy of every other three complexes to the σ-R in each medium. The Gap is the energy gap between HOMO and LUMO.

From the information in both table 2 and fig. 2, the reaction mechanism for the titled nitration can be illustrated as follows: First, the electrophilic agent, NO_2^+, attacks the area with high density of electron clouds, where it is across the benzene ring and between two carbons, to form a π complex of transition state (π-TS) by a low energy barrier of 2.744 kJ/mol. Then the nitronium ion shifts to one single carbon atom out of two equals, C_1 and C_6, to form a σ complex of reactant (σ-R), and the later via a σ-TS by activation energy of 8.370 kJ/mol to form the Wheland intermediate. Finally the σ-INT forms a nitrobenzene by releasing H^+ in a fast step. This is the situation in gas phase. The formation of σ-TS is the rate-determining step.

In solvents, however, the stabilization energy of σ-TS is much bigger than that of σ-R, since the dipole moment of former is much bigger than the later one. As a result, the activation energy of σ-TS is depressed more by the increasing dielectric constant of solvents. In the aqueous solution, the formation of σ-TS finally takes no barrier. The impact of solvents on the dipolar moment large complex σ-INT is the most drastic, especially on going from the vacant ($\varepsilon = 1$) to the nonpolar medium of $\varepsilon = 5$, and its stabilization energy has reached –21.10 kJ/mol. This means that the intrinsically endothermic nitration finally becomes an exothermic reaction in water (see fig. 2).

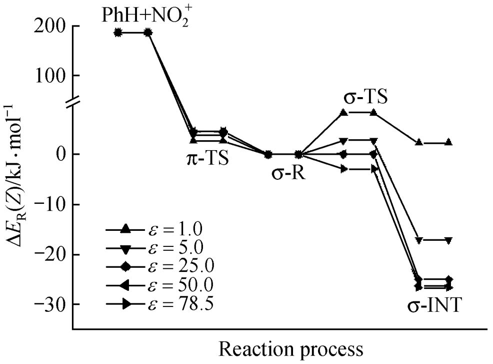

Fig. 2. Profile of nitration of PhH with NO_2^+ in different media at B3LYP/6-311G** level.

Besides a large amount of reports on electrophilic substitute mechanism, another electron transfer mechanism[1,2] involving radical pairs has been reported. We now compare these two mechanisms by our results both in thermodynamics and kinetics.

The energies and structures of two radicals of $PhH^{+\cdot}$ and $NO_2^{\cdot}$ were carried out by unrestricted B3LYP procedures at a 6-311G** level. Their total energies including ZPVE are –231.97468 and –205.10345 a.u., and the total energies of their molecule or ion are –232.30857 and –204.74901 a.u. respectively. Then the ionization potentials of the two radicals were calculated as 876.6 and 930.6 kJ/mol by the difference of total energy of the radical and the molecule or ion. Finally the energy for the electron transfer from benzene to NO_2^+ was carried out, –53.95 kJ/mol (–0.559 eV), which agrees with an experimental result of –0.55 eV[11], by the difference of ionization potentials (ΔE_R), where $\Delta E_R = E_f - E_s$, $E_s = E(\text{PhH}) + E(NO_2^+)$ and $E_f = E(\text{PhH}^{+\bullet}) + E(NO_2^\bullet)$. This means that the formation of two radicals from the initial reactants, benzene and NO_2^+, is energetically feasible. Yet the stabilization energies involving ZPVEs for four complexes were calculated by $\Delta E_{\text{stab}} = E_{\text{complex}} - (E_{\text{benzene}} + E_{NO_2^+})$, −184.7 (π-TS), −187.5 kJ/mol (σ-R), −179.1(σ-TS) and −185.1 kJ/mol (σ-INT) respectively, which are all even much lower than that of electron transfer. This shows that the formation of complex by electrophilic substitute is more favorable than that of radicals by electron transfer in the view of thermodynamics.

On the other hand, the inner sphere reorganization energy of NO_2^+ is very high, 128.8 kJ/mol (theoretical value[19]) or 109 kJ/mol (experimental value[2]) since the linear NO_2^+ bents significantly after an electron is transferred to. And the activation energy of the nitration is partly contributed by the reorganization energy of NO_2^+. So that, in the view of kinetics, there is little opportunity[20] of electron transfer using NO_2^+ as an oxidization agent for a nitration. And the electrophilic substitute is believed more favorable because its activation energy is only 8.370 kJ/mol in gas phase.

In a word, for both its high stabilization energies of complexes and low activation energy, the electrophilic substitute is considered here a more favorable mechanism than the electron transfer, at least for the titled nitration.

2.4 IR spectra

For the limitation of space, the IR spectra of only two complexes, σ-TS and σ-INT, significantly influenced by solvent effect, were discussed here. The dielectric constants of 1.0, 5.0 and 78.5 were used for the SCRF calculations to represent gas phase, nonpolar and aqueous solutions. Some vibration frequencies and intensities for bonds C_1-N_{13} and C_1-H_{12} are listed in table 4. From the intensities of the stretches, it is evident that the stretch of bond C_1-N_{13} is much stronger than that of bond C_1-H_{12}. In gas phase, there are several weak C-H stretches around 3200 cm^{-1} but a sharp one at 2919 cm^{-1}, which is the stretch of the bond C_1-H_{12}, between the attacked carbon and its hydrogen for leaving. And an out-of-plane bending vibration for this C-H is at 1084 cm^{-1}. An insignificant red shift found for bond C_1-H_{12} on going from σ-TS to σ-INT agrees with the slightly lengthening in bond length and the decreasing in bond order, showing that the bond C_1-H_{12} would not cleave in the Wheland intermediate, i.e. the formation of bond C_1-N_{13} and the cleavage of bond C_1-H_{12} are not cooperative but stepwise in the process of nitration. This is in full agreement with the fact that no kinetic isotope effect is observed in most aromatic nitrations. The stretches of bond C_1-N_{13} at 741 cm^{-1} in σ-TS and 817 cm^{-1} in σ-INT are very strong, showing that the bond

C_1-N_{13} has already partly formed in both σ-TS and σ-INT, and a blue shift for this bond on going from σ-TS to σ-INT reflects the tendency for its bond length to shorten and bond strength to increase (*vide ante*). Comparing the stretches of bond C_1-N_{13} of two stationary points in different media, the impact of solvent on its bond length, bond strength and blue shift from σ-TS to σ-INT shows that the polarity of solvent would benefit the formation and stabilization for both σ-TS and σ-INT complexes. It is worthy of noting that the calculated vibrational frequencies of two complexes presented here were not scaled but reliable since the computation by the B3LYP/6-311G** could often be used directly without scaling[21].

Table 4 Some vibration frequencies and intensities of bonds in the complexes of σ-TS and σ-INT at B3LYP/6-311G** level

	ε=1		ε=5		ε=78.5	
	σ-TS	σ-INT	σ-TS	σ-INT	σ-TS	σ-INT
Freq./cm^{-1}	740.9	816.7	749.4	832.7	825.3	834.1
IR inten./KM • mol^{-1}	329.2	293.8	324.8	170.8	143.9	156.4
Freq./cm^{-1}	3105.1	2918.9	3131.3	2891.9	2950.3	2889.2
IR inten./KM • mol^{-1}	26.7	62.4	23.7	74.2	73.4	76.2
Freq. /cm^{-1}	1081.8	1083.9	1098.1	1121.7	1134.2	1140.8
IR inten./KM • mol^{-1}	45.3	100.9	98.5	101.5	72.7	83.2

2.5 Thermodynamics and rate constant in gas phase

Based on the frequency analysis calculations, the standard thermodynamic functions of heat capacities (C_p^0), entropies (S_m^0) and enthalpies (H_m^0) for the σ-complexes of R and TS, as well as the change of entropy (ΔS_T) and the rate constant (k_A) for the rate-limiting step of titled reaction at each temperature were evaluated by using the theory of statistical thermodynamics, and then are listed in the table 5. It is evident that all the heat capacities and the rate constant (k_A) increase, whilst the change of entropy (ΔS_T) decreases, as expected, with increasing in temperature. It is worthy of noting that the rate constant (k_A) demonstrated here is in good agreement with an experimental rate constant of the order of 10^{10}mol • L^{-1} • s^{-1}[3].

Table 5 Thermodynamics for the rate-limiting step of the titled reaction

T/K	σ-complex R			σ-complex TS			ΔS_T/J • mol^{-1}• K^{-1}	$k_A \times 10^{-10}$/ mol^{-1} • s^{-1}
	C_p^0/J • mol^{-1}• K^{-1}	S_m^0/J • mol^{-1}• K^{-1}	H_m^0/kJ • mol^{-1} • K^{-1}	C_p^0/J • mol^{-1} • K^{-1}	S_m^0/J • mol^{-1}• K^{-1}	H_m^0/kJ • mol^{-1}• K^{-1}		
200.0	93.76	332.46	12.64	84.44	313.97	11.22	–18.49	0.294
298.2	128.50	376.28	23.52	119.06	354.02	21.18	–22.26	1.461
300.0	129.16	377.08	23.76	119.73	354.76	21.40	–22.32	1.489
400.0	163.73	419.06	38.44	154.61	394.07	35.15	–24.99	3.332
500.0	193.16	458.86	56.33	184.38	431.87	52.15	–26.99	5.417
600.0	216.98	496.26	76.88	208.47	467.70	71.84	–28.56	7.528
700.0	236.20	531.20	99.57	227.87	501.34	93.69	–29.86	9.545
800.0	251.91	563.80	124.01	243.71	532.84	117.29	–30.96	11.439

2.6 Linear correlations for the solvent effect on Wheland intermediate

Since the Wheland intermediate in a nitration is sometimes detectable in experiments, its geometry, electronic structure and other important properties, and how they behave in different media are both experimentally and theoretically concerned. So that, some properties of σ-INT impacted by the solvent polarities are specially discussed here. Hopefully, it would offer some referential data and their variations by media to the experimental works.

First, it was found that the solvent effect on the stabilization energy is in parallel with that on the net charges of NO_2 group for σ-INT. A linear relationship between the stabilization energies and the net charges of NO_2 group in the set of solvents is shown in fig. 3 (a). This means that the extra stabilization energy gained from the solvent by σ-INT is due to the strengthening charge migration from benzene to NO_2 group and the interaction between the two moieties by the solvent. Secondly, the dipole moment of the solute (σ-INT) is enlarged by the increasing solvent polarity. Therefore, another straight line is drawn in fig. 3 (b), the stabilization energies against the dipole moments of σ-INT in solvents. Combining the results of fig. 3 (a) and (b), it is obvious that the plot of dipole moments of σ-INT against the net charges of NO_2 group in the set of solvents should be also a straight line. That is, the stronger the solvent polarity, the more the negative charge left for NO_2 group, the bigger the dipole moment of solute, and the lower the stabilization energy ($\Delta E_{\mathrm{solv}}(Z)$). Similarly, a linear relation shown in fig. 3 (c) is found between the energy gap of frontier orbits and the dipole moments. The straight line shown in fig. 3 (d) then is the stabilization energies against the bond orders of C_1-N_{13}. Combining the results of (b), (c) and (d), a con-

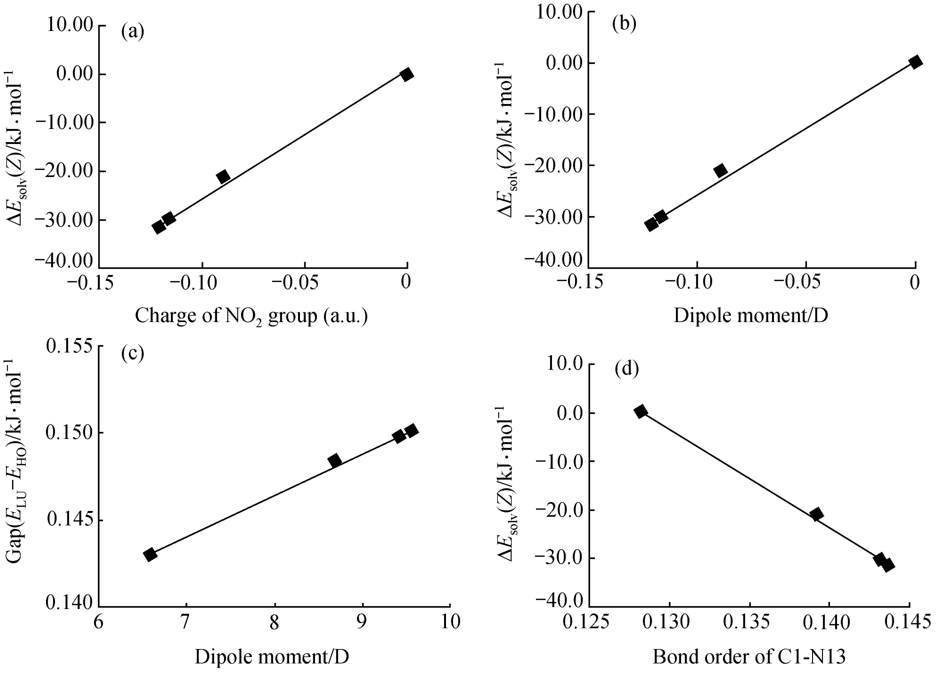

Fig. 3. Linear property-structure relations for Wheland intermediate in different media.

clusion could be drawn as follows: The energy gap is proportional to the stabilization energy; the bond order of C_1-N_{13} increases with the solvent polarity; both the bond order of C_1-N_{13} and the energy gap increasing finally lead to the elevation of the stabilization energy in solvents.

3 Conclusions

This paper reports the behaviors for the title reaction profile in different media at the B3LYP/6-311G** level, and the following conclusions can be reached:

(i) In gas phase, the electrophilic agent, NO_2^+, attacks a benzene ring to form four highly stabilized complexes of π-TS, σ-R, σ-TS and σ-INT one by one. The formation of σ-TS is the rate-determining step, and the activation energy is 8.37 kJ/mol. The order of rate constant is 10^{10}mol^{-1} • s^{-1}, in good agreement with an experimental observation.

(ii) For its high stabilization energies of complexes and low activation energy, the electrophilic substitute is considered here a more favorable mechanism than the electron transfer for the titled nitration in both thermodynamics and kinetics.

(iii) Since the dipole moment of σ-TS or σ-INT is much bigger than that of σ-R, as well as the stabilization energy, the activation energy is depressed by the solvent effect. The nitration in aqueous solution then undergoes without barrier and becomes an exothermic reaction from an intrinsically endothermic one. This is consistent with the experimental observation.

(iv) The formation of bond C_1-N_{13} and the cleavage of bond C_1-H_{12} are non-concerted stepwise. The absence of kinetic isotope effect for the nitration is then demonstrated by our results on geometries, charges, energetics and IR spectra.

(v) Linear property-structure relations for the experimentally detectible Wheland intermediate shows up the correlations between the bond order of C_1-N_{13}, the charge of NO_2 group, the dipole moment, the energy gap of frontier orbits and the stabilization energy in solvents in nature.

Acknowledgements L. Chen acknowledges a grant from the Science Center of Zhejiang University of Technology. This work was supported by the National Natural Science Foundation of China (Grant No. 20173028).

References

1. Perrin, C. L., Necessity of electron transfer and a radical pair in the nitration of reactive aromatics, J. Am. Chem. Soc., 1977, 99: 5516—5518.
2. Eberson, L., Hartshorn, M. P., Radner, F., Ingold's nitration mechanism lives, Acta Chem. Scand., 1994, 48: 937—950.
3. Schofield, K., Aromatic Nitration, London, New York: Cambridge Univ. Press, 1980.
4. Politzer, P., Jayasuriya, K., Sjoberg, P. et al., Properties of some possible intermediate stages in the nitration of benzene and toluene, J. Am. Chem. Soc., 1985, 107: 1174—1177.
5. Gleghorn, J. T., Torossian, G. (in part), Theoretical study of the enthylene and benzene with the nitronium ion, J. Chem. Soc. Perkin Trans., II, 1987: 1303—1310.
6. Szabo, K. J., Hornfeldt, A. -B., Gronowitz, S., Theoretical study on mechanism and selectivity of electrophilic aromatic nitration, J. Am. Chem. Soc., 1992, 114: 6827—6834.
7. Melander, L., Saunders, W. H. Jr., Reactions Rates of Isotopic Molecules, New York: John Wiley and Sons, 1980.
8. Wheland, G. W., A quantum mechanism investigation of the orientation of substituents in aromatic molecules, J. Am. Chem. Soc., 1942, 64: 900—909.

9. Harmond, G. S., A correlation of reaction rates, J. Am. Chem. Soc., 1955, 77: 334—338.
10. Weast, R. C., Handbook of Chemistry and Physics, 55th ed., Cleveland: CRC Press, 1974.
11. Xiao, H. M., The Molecular Orbital Theory for Nitro Compounds, Beijing: National Defense Industry Press, 1993.
12. Xiao, H. M., Chen, Z. X., The Modern Theory for Tetrazol Chemistry, Beijing: Science Press, 2000.
13. Zhang, J., Xiao, H. M., Gong, X. D., Theoretical studies on heats of formation for polynitrocubanes using the density functional theory B3LYP methods and semiempirical MO methods, J. Phys. Org. Chem., 2001, 14: 583—588.
14. Li, J. S., Xiao, H. M., Dong, H. S., A theoretical study on the intermolecular interaction of energetic system——Nitromethane dimmer, Chin. J. Chem., 2000, 18(6): 815—819.
15. Zhang, J., Xiao, H. M., Computational studies on the infrared vibrational spectra, thermodynamic properties, detonation properties, and pyrolysis mechanism of octanitrocubane, J. Chem. Phys., 2002, 116: 10674—11683.
16. Seminario, J. M., Politzer, P., Modern Density Functional Theory: A Tool for Chemistry, Amsterdam: Elsevier, 1995.
17. Frisch, M. J., Trucks, G. W., Schlegel, H. B., et al., Gaussian 98w on-line help.
18. Wong, M. W., Frisch, M. J., Wiberg, K. B., Solvent effects, 1. The mediation of electrostatic effects by solvents, J. Am. Chem. Soc., 1991, 13: 4776—4791.
19. Li, X. Y., He, F. C., Electron transfer $NO_2^+ + NO \rightarrow NO_2 + NO^+$ in aromatic nitration, Science in China, Series B, 1997, 40(5): 523—528.
20. Mu, T. C., Zhou, L. Z., Calculation reorganization energy of electron transfer reaction in benzene nitride, Chin. J. Chem. Phys., 2002, 15(5): 363—366.
21. Scott, P., Radom, L., Harmonic vibrational frequencies: An evaluation of Hartree-Fock, moller-plesset, quadratic configuration, density functional theory and semiempirical scale factor, J. Phys. Chem., 1996, 100: 16502—16513.